Prediction of elastic properties for polymer–particle nanocomposites exhibiting an interphase

Prediction of elastic properties for polymer–particle nanocomposites exhibiting an interphase

Fei Deng and Krystyn J Van Vliet[1]

Department of Materials Science and Engineering, Massachusetts Institute of Technology,
Cambridge, MA 02139, USA

E-mail: krystyn@mit.edu

Abstract
Particle–polymer nanocomposites often exhibit mechanical properties described poorly by
micromechanical models that include only the particle and matrix phases. Existence of an
interfacial region between the particle and matrix, or interphase, has been posited and indirectly
demonstrated to account for this effect. Here, we present a straightforward analytical approach
to estimate effective elastic properties of composites comprising particles encapsulated by an
interphase of finite thickness and distinct elastic properties. This explicit solution can treat
nanocomposites that comprise either physically isolated nanoparticles or agglomerates of such
nanoparticles; the same framework can also treat physically isolated nanoparticle aggregates or
agglomerates of such aggregates. We find that the predicted elastic moduli agree with
experiments for three types of particle–polymer nanocomposites, and that the predicted
interphase thickness and stiffness of carbon black–rubber nanocomposites are consistent with
measured values. Finally, we discuss the relative influence of the particle–polymer interphase
thickness and stiffness to identify maximum possible changes in the macroscale elastic
properties of such materials.

(Some figures in this article are in colour only in the electronic version)

1. Introduction

For a range of polymer composites comprising particle fillers,
it has been posited that an interphase region [1, 2] of
nanometre-scale thickness t arises due to complex interactions
at the particle–polymer matrix interface [3]. For filler
particles of $>\mu$m-scale radius r, the contribution of such a
thin interphase to the elastic properties of the composite is
negligible. However, for particles of nm-scale radius, this
potential contribution increases due to increased interfacial
surface area [4–8]. For example, for $t/r = 0.5$, the interphase
volume fraction exceeds 200% of the particle volume fraction,
such that the macroscale elastic properties are expected to be
dominated by those of both the particles and the interphases.

Consequently, analytical treatment of composites com-
prising interphases has received significant attention. For

example, Lutz and Zimmerman [9] and Weng and Ding [10]
explored the mechanical contributions of an interphase by
solving for the stress field and effective bulk moduli of
composites containing spherical particles, embedded within
inhomogeneous matrices that exhibited a particle distance-
dependent power law gradation in elastic moduli. Herve and
Zaoui [11] proposed a model with an n-layered spherical
inclusion embedded in an infinite matrix, and Nie and
Basaran [12] instead replaced the particle–interphase region
with an effective particle; both groups applied hydrostatic
pressure and simple shear to obtain a series of parameterized
equations from which bulk and shear elastic moduli could
be calculated. However, for nearly all the existing analytical
models of composite homogenization, predictions of elastic
properties were obtained by solving the elastic governing
equations under those specific applied stress states [9–12]. As
a result, the expressions for the elastic constants are highly
parameterized and coupled, such that one must iteratively infer

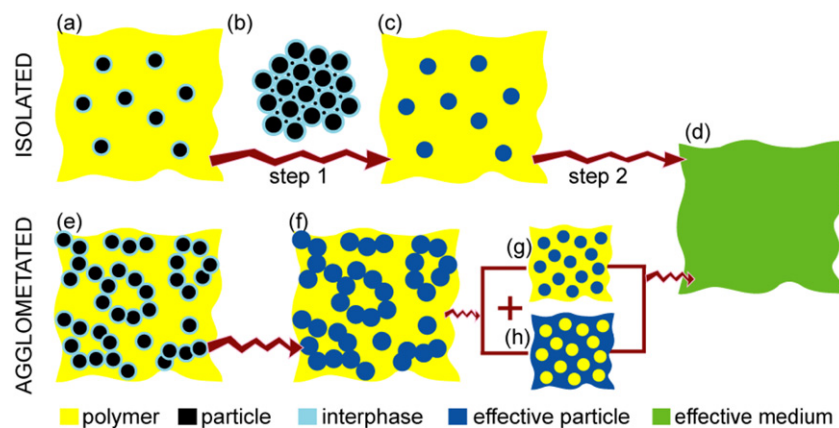[1] Author to whom any correspondence should be addressed.

Figure 1. Schematic method to estimate the elastic properties of a composite comprising particles surrounded by interphases. (a) For low volume particle volume fractions approximating the dilute limit, the actual composite comprises particles surrounded by interphases that are embedded within a matrix. (b) The elastic properties of the effective particle are obtained by representing this phase via an infinite volume that is fully packed with particle–interphase regions of decreasing diameter and identical shape. (c) The particle–interphase regions are mechanically equated to effective particles in a polymer matrix. (d) The macroscale composite is represented by an effective medium that is strain energy equivalent to the effective particle–matrix composite. (e) For high particle volume fractions or strong particle–interphase–particle interactions, agglomeration of nanoparticles may occur. The topology of the composite is such that the polymer may surround interphase-encapsulated nanoparticles, or the interphase-encapsulated nanoparticles may surround the polymer. In other words, no one phase fully encompasses the other phase. The particle region shown in (e) can in fact represent a single nanoparticle or aggregates of such nanoparticles; aggregates may be physically isolated or agglomerated. (f) The particle–interphase (or aggregate–interphase) regions are mechanically equated to effective particles. To create the effective medium (d), the elastic properties of (f) are represented by a weighted volume fraction of the polymer matrix, where (g) is the polymer acting as a continuous matrix around isolated effective particles, and (h) is the effective particles acting as a continuous matrix around isolated polymer inclusions.

the effects of interphase stiffness, thickness, or particle volume fraction on the composite response. Further, such approaches generally require new analytical derivations for changes in particle shape. More importantly for the consideration of nanocomposites, the nature of these analytical approaches is constrained to the dilute limit of physically isolated particles. In actuality, the high relative surface area of nanoparticles often promotes aggregation or agglomeration at higher particle volume fractions, which is incommensurate with the assumptions of these analytical approaches.

Here, we describe a straightforward method to estimate the effective elastic properties of composites comprising spherical particles surrounded by mechanically distinct interphases, explicitly in terms of the elastic properties and physical dimensions of the particle–polymer composite. We show that this approach can be applied to nanocomposites comprising a low volume fraction of well-dispersed and spatially isolated nanoparticles, as well as nanocomposites comprising regions of agglomerated nanoparticles; these agglomerated regions exhibit complex geometries that may encapsulate the polymer matrix. Depending on the details of the particle–polymer interactions and volume fraction of nanoparticles, particles may aggregate to form geometrically self-similar regions surrounded by interphases; this same approach can also be applied to nanocomposites comprising well-dispersed nanoparticle aggregates and to agglomerates of those aggregates. Application of our model to experimental measurements for oxide nanoparticle–epoxy nanocomposites and to carbon black nanoparticle–elastomer nanocomposites shows good agreement in the prediction of macroscale elastic moduli. Further, prediction of the interphase thickness and

elastic properties agrees well with available measurements for elastomeric nanocomposites. This explicit relation between interphase and macroscale properties also elucidates the relative contributions of interphase thickness and stiffness to macroscopic elastic moduli, aiding the design of nanoparticles and nanocomposites for optimized mechanical performance.

2. Theoretical model

Figure 1 schematizes the theoretical model by which we relate the nanocomposite properties to those of the constituent phases, for both the isolated and the agglomerated cases. We treat spherical nanoparticles as our case of interest and for comparison with experiments; other particle geometries such as ellipses and tubes can be easily accommodated through this same approach, by replacing the corresponding Eshelby tensor of the particle inclusion [13–15]. Further, we note that this general approach is not restricted to particles of nanoscale diameter, but is discussed here in terms of nanoparticles because the potential mechanical contributions of nanometres-thick interphases are much greater in particle–polymer nanocomposites as compared to micro- or macrocomposite materials.

To describe the nanoparticle–interphase–matrix composite, we approximate all particles to be of radius r and interphase thickness t. The nanoparticle–interphase regions are thus represented as core–shell structures embedded in an infinite matrix. All interfaces between particles and interphases and between interphases and the surrounding matrix are assumed perfectly bonded, whereby complexities

such as macromolecular chain entanglement or imperfect bonding are reflected in the apparent elastic properties of the interphase. This description assumes the mechanical differences between the nanoparticle and matrix to exist over a relatively sharp and finite region, conceptualizing this transition as an actual 'interphase' or distinct annulus of defined nm-scale thickness and elastic properties. This approximation is consistent with recent experiments visualizing mechanically distinct interphases surrounding particles in elastomers [16, 17]. However, we note that in actual polymeric nanocomposites, the relative contributions of these interactions and the uniformity of interphase thickness depend on particle and polymer chemistries, processing details, and physical environments [18, 19].

2.1. Isolated case

For nanocomposites of low nanoparticle volume fraction, which we term the isolated case, the particles can be well dispersed and thus the particle–interphase regions are physically isolated (figure 1(a)). In this isolated case, estimation of the effective elastic properties of the composite then pivots on two steps. First, the particle–interphase region is replaced (figure 1(b)) by an effective particle of identical size and shape (figure 1(c)). The elastic properties of the effective particle and particle–interphase structure are energetically equivalent, such that the stored elastic strain energies of these regions should be equivalent for a given stress. In other words, the elastic properties of these effective particles are represented by an effective particle medium (figure 1(b)) comprising only the particle–interphase regions; this medium is constructed by filling the space between optimally packed particle–interphase regions completely with particle–interphase regions of decreasing diameters. This effective particle medium is required to calculate the elastic properties of the classical inclusion-infinite matrix composite: micromechanical inclusion models assume an infinite matrix, but the interphase representation as a shell is finite. In contrast to previous analytical models that solve the elastic governing equations under specific boundary conditions [11, 12], here we obtain the elastic constants of the effective particles by incorporating these within a composite system. Figure 1(b) can then be regarded as a composite system (particles as inclusions and interphase material as matrix) possessing the same elastic properties as the particle–interphase structures and as the effective particles. In the second step required to represent the macroscopic response of the nanocomposite material, the composite comprising the effective particles is represented by a homogeneous effective medium (figure 1(d)).

The elastic properties of effective particles can thus be directly obtained by existing micromechanical estimations. We adopt the interaction direct derivation (IDD) [13, 14, 20] because of its high accuracy in consideration of inclusion interactions. For the elastically isotropic particle and interphase, the bulk modulus K_{EP} and shear modulus G_{EP} of

the effective particles are represented as

$$K_{EP} = K_I \left(1 + \frac{(K_I/K_P - 1)a}{1 + \eta_I(1 - a)(1 - 2v_I)(K_I/K_P - 1)} \right)^{-1}$$

$$G_{EP} = G_I \left(1 + \frac{(G_I/G_P - 1)a}{1 + \delta_I(1 - a)(1 + v_I)(G_I/G_P - 1)} \right)^{-1}$$

(1)

where v is Poisson's ratio, K is the bulk modulus, G is the shear modulus, and the subscripts I and P denote the interphase and particle, respectively. The parameters η_I and δ_I reflect the Eshelby tensor of the particle; for spherical particles, $\eta_I = 2/(3(1 - v_I))$ and $\delta_I = (7 - 5v_I)/(15(1 - v_I^2))$. The volume fractions of the particle and interphase are f_P and f_I, respectively. In the particle–interphase extended region (figure 1(b)), the volume fraction of the particle in (b) is then $a = f_P/(f_I + f_P) = (r/(t + r))^3$. Note that for nanocomposites in which the interphase elastic properties vary over a considerable distance according to a specified function, differential techniques [21] can be applied to obtain the elastic moduli of the effective particle based on equation (1).

At low nanoparticle volume fractions, the elastic constants of the entire nanocomposite (K, G) or (E, v) shown in figure 1(d) can also be obtained by equation (1). In this dilute limit, this nanocomposite comprises isolated effective particles within a matrix, of volume fraction $f_{EP} = f_I + f_P = f_P/a$. In this application of equation (1), the particle properties (K_P, G_P, v_P, a) are replaced with those of the effective particles $(K_{EP}, G_{EP}, v_{EP}, f_{EP})$, and the interphase properties (K_I, G_I, v_I) are replaced with those of the matrix (K_m, G_m, v_m). Since the effective particles are also spherical, the parameters η_I and δ_I are changed to η_m and δ_m by replacing v_I with v_m. The elastic constants (K, G) of the nanocomposite at low volume fraction are obtained as follows:

$$K = K_m \left(1 + \frac{(K_m/K_{EP} - 1)f_{EP}}{1 + \eta_m(1 - f_{EP})(1 - 2v_m)(K_m/K_{EP} - 1)} \right)^{-1}$$

$$G = G_m \left(1 + \frac{(G_m/G_{EP} - 1)f_{EP}}{1 + \delta_m(1 - f_{EP})(1 + v_m)(G_m/G_{EP} - 1)} \right)^{-1}.$$

(2)

To compare with experiments that typically report E and v, we extend the assumption of elastic isotropy to calculate Young's modulus $E = 9KG/(3K + G)$ and $v = (3K - 2G)/(6K + 2G)$.

At increased volume fraction of nanoparticles, significant aggregation may occur. Note that if these aggregates are highly dispersed and isolated from each other, this 'isolated nanoparticle' framework is also applicable; the nanoparticles in figure 1(a) would then be represented by the dimensions and elastic properties of these aggregates.

2.2. Agglomerated case

The above results are based on the assumption that interphase-encapsulated nanoparticles are physically isolated from each other. In fact, the isolated case can also describe nanocomposites comprising aggregates of nanoparticles, wherein each aggregate is encapsulated by an interphase and is

physically isolated from other such aggregates via the matrix. As the nanoparticle volume fraction increases or the particle–polymer interactions are modified, however, interphase-encapsulated nanoparticles and nanoparticle aggregates may exhibit close spatial proximity. In such cases, the potential for connectivity among nanoparticle aggregates (or among nanoparticles) via the interphase breaks the concept of geometric self-similarity that is inherent to the isolated case; see figure 1(e). This connectivity among aggregates is sometimes termed agglomeration [22]. We thus refer to this as the agglomerated case, which implies a physical connectivity among the interphase-encapsulated fillers that is geometrically complex (i.e., dissimilar from the nanoparticle shape or resulting in closed paths that occlude the polymer matrix). In this configuration, the topology of the composite is such that some regions may comprise nanoparticle aggregates (or nanoparticles) surrounded by polymer, and other regions may comprise polymer surrounded by these nanoparticle aggregates (or nanoparticles). In other words, no one phase fully encompasses the other phases [17]. The effective particles in the agglomerated case are mechanically equivalent to the interphase-encapsulated nanoparticle aggregates (or the interphase-encapsulated nanoparticles), as indicated in figure 1(f). The connectivity among such nanoparticle aggregates (or among such nanoparticles) via the interphase between them and around them enables this equivalence to such an effective particle domain.

In this agglomerated case (figures 1(e) and (f)), the topology of the composite is such that one phase does not fully encompass the other phase, and does not require an assumption of full percolation of either phase. For such complex composite morphologies, other micromechanical modelling approaches such as the self-consistent method (SCM) can be considered. However the solutions of that approach are implicit, and this renders the SCM inappropriate for studies seeking to infer interphase properties of phase thickness and stiffness via macroscale characterization of the composite elastic modulus. Here, we treat the polymer and the effective particles in the same manner (figures 1(g) and (h)). Figure 1(g) represents the elastic response of the polymer acting as a matrix that surrounds the effective particles; figure 1(h) represents the elastic response of the effective particles acting as a phase that surrounds the polymer inclusions. To smoothly connect these two extreme cases and thus treat the intermediate agglomerated case, we adopt the Voigt approximation as a linear superposition weighted by the phase volume fraction. The stiffness tensor of the composite is then a weighted summation of the stiffness tensors of these two extremes, according to the volume fraction of the polymer matrix (for figure 1(g)) and of the effective particles (for figure 1(h)). Thus, the elastic properties of the nanocomposite in the agglomerated case (E_{agg}, v_{agg}) are obtained as follows:

$$K_{agg} = (1 - f_{EP})K + f_{EP}K' \qquad G_{agg} = (1 - f_{EP})G + f_{EP}G'.$$
$$(3)$$

Here (K, G) are the elastic constants of the effective medium given by the isolated case where the polymer surrounds the effective particle inclusions in figure 1(g). The elastic constants (K', G') represent the effective medium given by the extreme where the effective particles surround the polymer inclusions in figure 1(h). Note that the process to calculate (K, G) and (K', G') is identical to that given in the discussion of equation (2), except that the polymer and particle subscripts are replaced with the appropriate surrounding phase and inclusion phase subscripts. The corresponding Young's modulus of the composite for the agglomerated case E_{agg} is also calculated from the bulk and shear moduli as $E_{agg} = 9K_{agg}G_{agg}/(3K_{agg} + G_{agg})$. We note that aggregation and/or agglomeration will lead to local anisotropy in the elastic response, but that the macroscopic elastic properties of the nanocomposite are reasonably assumed to be isotropic if the aggregates or agglomerates are distributed homogeneously and of average physical dimensions much less than the sample dimensions.

3. Results and discussion

We first applied this model to the reported macroscale measurements of Young's elastic moduli E for three types of nanocomposites comprising small nanoparticle volume fractions (<10 vol% of either Al_2O_3 or TiO_2 nanoparticles in an epoxy matrix). Figure 2(a) shows experimentally measured $E_{composite}$ for these three oxide nanoparticle–epoxy composites, each measured over a range of particle volume fractions [23–25]. Over this range of low volume fractions, such particles are generally well dispersed and the isolated model framework (see figure 1(a) and equation (2)) can be reasonably assumed. Our model requires input of the matrix and particle elastic constants, and of the particle radius; these were reported in [23–25] as indicated in the caption of figure 2. If the existence of an interphase region is neglected entirely, our model comprising only the epoxy and oxide phases (represented in figure 2(a) as dashed lines) poorly fits each of these experimental systems. We assumed an interphase of uniform elastic properties to exist, as there is no reported information quantifying gradients in such epoxy interphase properties, and that these elastic properties differed from those of both the polymer matrix and the oxide particles. Best fitting of our model to each of these three nanocomposite systems gives predictions of the measured composite modulus when an interphase of fitted thickness and stiffness is included (solid lines). The values of interphase thickness t and elastic modulus E_I were obtained via the best fit of this model (i.e., the set (t, E_I) obtained via least squares nonlinear regression with respect to the measured $E_{composite}$) for each of these three composites. We find that $t = 36$ nm and $E_I = 40$ GPa for alumina–epoxy nanocomposite 1 [23]; $t = 10$ nm and $E_I = 30$ GPa for alumina–epoxy nanocomposite 2 [24]; and $t = 19$ nm and $E_I = 22$ GPa for the titanium oxide–epoxy nanocomposite [25]. Thus, it is consistently predicted that the interphase region is approximately one order of magnitude stiffer than the bulk epoxy. Although no direct measurement of interphase thickness or stiffness has been reported for these composites, indirect estimates from a range of experiments also suggest this level of interphase stiffening and thickness [26, 27].
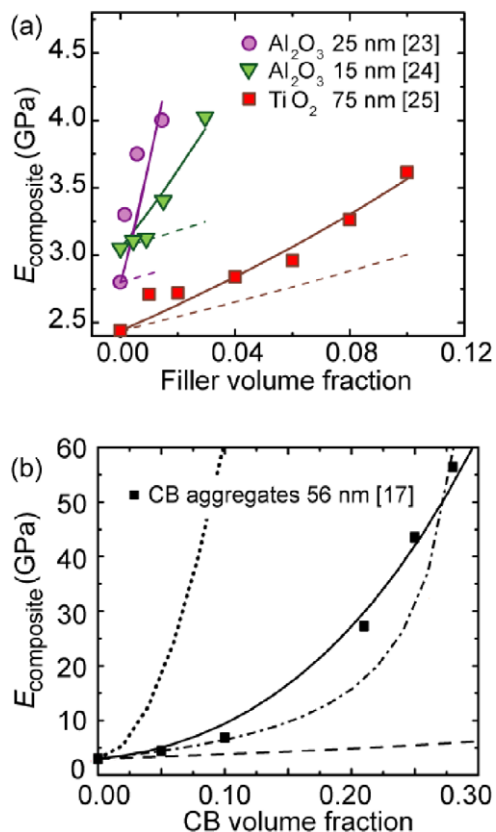
Figure 2. Comparison of Young's modulus as measured experimentally (points) and estimated from the present model (lines), for two classes of polymer–particle composites. (a) Results for oxide nanoparticle–epoxy composites from [23–25], with nanoparticle radius indicated in the legend. The elastic properties (Young's modulus and Poisson's ratio) of the particle and matrix phases were assumed as $E_{TiO_2} = 283$ GPa and $\nu_{TiO_2} = 0.28$, $E_{Al_2O_3} = 283$ GPa and $\nu_{Al_2O_3} = 0.24$; E_m of the epoxy matrices was taken from the corresponding measured values reported in [23–25], and ν_m of the epoxy was assumed as 0.364. The dashed lines are theoretically estimated $E_{composite}$ using the isolated nanoparticle model in the absence of an assumed interphase. The solid lines are $E_{composite}$ when an assumed interphase is included in the isolated nanoparticle model. The magnitudes of interphase thickness and stiffness corresponding to the best-fit nonlinear regressions to these data for each composite system are indicated in the text. (b) Results for hydrogenated nitrile butadiene rubber (HNBR)–carbon black nanocomposite at 35 °C from [17] indicate nonlinear increases with increasing carbon black volume fraction. The carbon black aggregate diameter was reported as 56 nm in experiments [17]. The elastic modulus of the HNBR matrix was reported as $E_{HNBR} = 3$ MPa in [17], and ν_{HNBR} was assumed as 0.499; the elastic properties of CB were assumed as equivalent to graphite, $E_{CB} = 10$ GPa and $\nu_{CB} = 0.3$. The dashed line indicates model predictions in the absence of an interphase and absence of effective particle and CB nanoparticle contact (no interphase in the isolated case); the dash-dotted line indicates model predictions in the presence of an interphase and absence of agglomeration (isolated interphase-encapsulated nanoparticle aggregate) with fitted interphase thickness $t = 26$ nm and stiffness $E_{BR} = 580$ MPa; the dotted line indicates model predictions in the absence of an interphase and the presence of CB nanoparticle contact (extreme agglomerated case with no interphase); and the solid line indicates model predictions in the presence of an interphase that surrounds each nanoparticle aggregate (agglomerated case consistent with experiments) with fitted interphase thickness $t = 22$ nm and stiffness $E_{BR} = 37$ MPa. The magnitudes of interphase thickness and stiffness corresponding to the best-fit solid line are indicated in the text.

We also applied this theoretical model to carbon black–rubber nanocomposites comprising up to 28 vol% carbon black (CB) nanoparticles. For such high volume fractions of carbon black in this hydrogenated nitrile butadiene rubber (HNBR)-matrix, particle aggregation and agglomeration are typically observed [16, 17]. To efficiently cover the entire compositional range, the agglomerated case framework (see figure 1(e) and equation (3)) is advantageous. We note that the numerical predictions of the agglomerated case will approach those of the isolated case at very low nanoparticle volume fractions ($f_P \rightarrow 0$). In these CB–rubber nanocomposites, the concept of a 'bound rubber' interphase of distinct elastic modulus has been widely postulated and inferred from both mechanical and thermal analyses [17, 22]. Although the HNBR matrix elastic properties and the carbon black aggregation diameter are experimentally measured and reported (figure 2), the elastic constants of carbon black (E_{CB}, ν_{CB}) are not well defined experimentally; here, those of graphite were assumed ($E_{CB} = 10$ GPa, $\nu_{CB} = 0.3$). Figure 2(b) shows successful agreement of theoretical results and these experimental data. We find that $t = 22$ nm and $E_{BR} = 37$ MPa, via a best-fit nonlinear regression to the measured $E_{composite}$. Moreover, the interphase thickness and Young's elastic modulus can be computed as a range over which this nonlinear increase of $E_{composite}$ with increasing vol% carbon black is a reasonably good fit (R^2 optimization criterion $0.97 < R^2 < 1$); we then obtain as a range 30 MPa $< E_{BR} <$ 58 MPa for corresponding interphase thickness t ranging from 27 to 14 nm. (In other words, this best-fit stiffness and thickness of the interphase is within a narrow range of more compliant/thicker interphases and stiffer/thinner interphases.) Note that this best fitting of the model does not bound or require the stiffness of the interphase to be greater than that of the matrix or less than that of the carbon black nanoparticle aggregates. Importantly, both the best-fit and this range of interphase stiffness and thickness agree well with that measured experimentally via torsional harmonic AFM imaging and mechanical analysis ($E_{BR} = 53 \pm 11$ MPa and $t = 19 \pm 8$ nm [17]). Here, we remark that in the agglomerated case appropriate for this elastomeric nanocomposite, the presence of an interphase is widely hypothesized and is supported by other extremes that can be tested by this model. For example, in the absence of a mechanically dissimilar interphase and the absence of nanoparticle contact, the composite would revert to the isolated and interphase-free nanoparticle model (dashed line, which underpredicts the measured composite stiffness). Conversely, in the absence of an interphase and under the assumption that the CB nanoparticles are in direct mechanical contact, the composite would be much stiffer than observed experimentally (dotted line). In such a prediction, the agglomerated case framework is applied by equating the nanoparticle aggregates with the effective particles. Further, if we assume the presence of interphase and absence of agglomeration (dashed-dotted line), the best-fit interphase thickness and stiffness values are $t = 26$ nm and $E_{BR} = 580$ MPa. As this interphase stiffness is one order of magnitude greater than that measured experimentally [17], this indicates that the assumption of isolated, interphase-surrounded nanoparticle aggregates is not

applicable in this particular case of high nanoparticle volume fraction nanocomposites. However, if we assume that the nanoparticle aggregates are surrounded by an interphase and that these interphase-encapsulated aggregates are partially agglomerated, our model (solid line) successfully captures the experimental trend and the magnitudes of both interphase stiffness and thickness ($t = 22$ nm and $E_{BR} = 37$ MPa).

We note that the agglomerated case can seamlessly span very low and very high levels of agglomeration (of nanoparticles or of aggregates). However, this case does not include the possibility that some nanoparticles are aggregated (or that some aggregates are agglomerated) while other nanoparticles (or aggregates thereof) are isolated. If one is interested in explicitly treating a range of aggregate diameters, including individual nanoparticles coexisting with aggregated nanoparticles, this is fully accessible via a modification of the isolated case described above. Briefly, equation (1) can be integrated with respect to effective particle diameter over the limits of interest [20]. This could be implemented as a weighted sum of discrete average diameters of the effective particles, and the interphase thickness would be assumed invariant with effective particle diameter. However, connectivity among the interphase-encapsulated aggregates (agglomeration) would not be accessible with this approach. Thus, if one's nanocomposite of interest exhibits such agglomeration among aggregates (or among nanoparticles), the agglomerated model is applicable.

Beyond the prediction of a given nanocomposite's interphase existence, thickness, and stiffness, this model also provides a means to quantify how further changes in the interphase thickness or stiffness surrounding dispersed nanoparticles would alter the composite elastic modulus. To consider the relative effects of interphase thickness and stiffness on the nanocomposite elastic modulus, we systematically varied t or E_I using the isolated case framework as an example. Figure 3(a) summarizes the effect of varied relative interphase stiffness E_I/E_P for a constant relative interphase thickness t/r. Figure 3(b) summarizes the effect of varied interphase thickness t/r for constant E_I/E_P. As anticipated, an increase in either interphase thickness or Young's modulus increases the elastic modulus of the composite in a nonlinear fashion. This comparison also makes it clear that stiffening of the interphase is characterized by descending reinforcement, whereas thickening of the interphase is characterized by ascending reinforcement. That is, for a given interphase thickness, increases in E_I lead to a rapidly saturating stiffness of the composite. In contrast, for a given interphase stiffness, further increases in t lead to increasing rates of stiffening at the composite level. Of course, the maximum interphase thickness is limited by the particle volume fraction as $(1 + t/r)^3 < 1/f_P$. In practice, for a given polymer–particle nanocomposite it may not be possible to significantly modify the interphase thickness or stiffness (e.g., through variation of particle surface chemistry or polymer matrix reactivity [28]). However, the parameterization represented in figure 3 allows one to determine whether the experimentally attainable variation in either E_I or t will achieve the desired macroscopic stiffening of such nanocomposites.
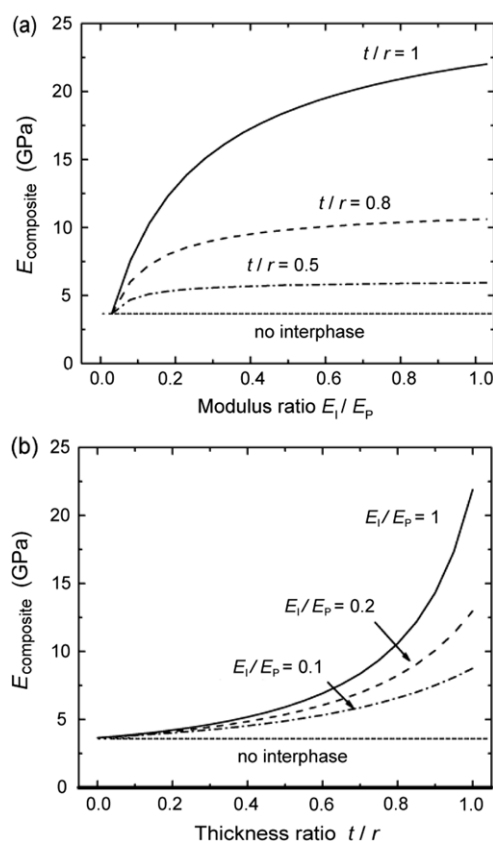

Figure 3. The effects of the interphase Young's modulus and thickness on the Young's modulus of the nanocomposite, as determined for the isolated case described in the text. (a) Interphase stiffness relative to particle stiffness E_I/E_P is varied for a given relative interphase thickness t/r. (b) Interphase thickness relative to particle radius t/r is varied for a given relative interphase stiffness. The mechanical contribution of the interphase decreases with increasing relative interphase stiffness E_I/E_P, and increases along with increasing normalized interphase thickness t/r. In both (a) and (b), the elastic constants of the matrix and particles were assumed as $E_m = 3$ GPa, $E_P = 100$ GPa, and $\nu_m = \nu_P = 0.36$.

Given that both the isolated case and the agglomerated case were demonstrated to work well for specific examples, one may question which model to implement for his/her nanocomposite of interest. Here, the choice lies not in the range of nanoparticle volume fraction considered, but rather in the composite microstructure. If agglomeration among the nanoparticles or among the aggregates is observed, then the agglomerated case should be implemented; this could occur for even low nanoparticle volume fractions due to complexities among particle–particle and particle–matrix interactions. The connectivity and loss of geometric self-similarity in such agglomerations cannot be treated by the isolated case. Thus, inspection of the final composite microstructure (e.g., via transmission electron microscopy or tomography) will aid in the appropriate choice of model for such predictions of interphase-dependent elastic properties.

4. Conclusions

In conclusion, an analytical approach is proposed to estimate the elastic properties of particle-reinforced nanocomposites

that exhibit potential mechanical contributions from the particle–polymer interphase. This approach provides explicit solutions to predict the stiffness and thickness of the interphase from measurements of the macroscopic elastic moduli of the composites. Successful agreement is shown for particle–polymer nanocomposites in which the nanoparticles or particle aggregates are well dispersed and physically isolated from each other, and for nanocomposites in which the nanoparticles or nanoparticle aggregates may locally surround the polymer phase. Furthermore, the relative contributions of interphase thickness and stiffness are compared for composites comprising well-dispersed nanoparticles, demonstrating how the mechanical contributions of such an interphase vary nonlinearly with increasing volume fraction or elastic modulus of the interphase. Applications of this tractable model can thus enable the design of polymer nanocomposites and polymer–particle interphases with anticipated elastic properties.

References

[1] Stickney P B and Falb R D 1964 *Rubber Chem. Technol.* **37** 1299–340
[2] Drzal L T 1990 *Vacuum* **41** 1615–8
[3] Tzika P A, Boyce M C and Parks D M 2000 *J. Mech. Phys. Solids* **48** 1893–929
[4] Brown D, Mele P, Marceau S and Alberola N D 2003 *Macromolecules* **36** 1395–406
[5] Thostenson E T, Li W Z, Wang D Z, Ren Z F and Chou T W 2002 *J. Appl. Phys.* **91** 6034–7
[6] Mahfuz H, Hasan M, Dhanak V, Beamson G, Stewart J, Rangari V, Wei X, Khabashesku V and Jeelani S 2008 *Nanotechnology* **19** 445702
[7] Diez-Pascual A M *et al* 2009 *Nanotechnology* **20** 315707
[8] Cai D Y, Yusoh K and Song M 2009 *Nanotechnology* **20** 085712
[9] Lutz M P and Zimmerman R W 1996 *J. Appl. Mech.-Trans. ASME* **63** 855–61
[10] Ding K and Weng G J 1998 *J. Elast.* **53** 1–22
[11] Herve E and Zaoui A 1993 *Int. J. Eng. Sci.* **31** 1–10
[12] Nie S H and Basaran C 2005 *Int. J. Solids Struct.* **42** 4179–91
[13] Deng F and Zheng Q S 2008 *Appl. Phys. Lett.* **92** 071902
[14] Deng F, Zheng Q S, Wang L F and Nan C W 2007 *Appl. Phys. Lett.* **90** 021914
[15] Mura T 1987 *Micromechanics of Defects in Solids* 2nd edn (Dordrecht: Martinus Nijhoff Publishers)
[16] Berriot J, Martin F, Montes H, Monnerie L and Sotta P 2003 *Polymer* **44** 1437–47
[17] Qu M, Deng F, Kalkhoran Salmon M, Gouldstone A, Robisson A and Van Vliet K J 2011 *Soft Matter* **7** 1066–77
[18] Paul D R and Robeson L M 2008 *Polymer* **49** 3187–204
[19] Druffel T, Lattis M, Spencer M and Buazza O 2010 *Nanotechnology* **21** 105708
[20] Zheng Q S and Du D X 2001 *J. Mech. Phys. Solids* **49** 2765–88
[21] Shen L X and Li J 2003 *Int. J. Solids Struct.* **40** 1393–409
[22] Robisson A 2010 *Mech. Mater.* **42** 974–80
[23] Omrani A, Simon L C and Rostami A A 2009 *Mater. Chem. Phys.* **114** 145–50
[24] Zhao H X and Li R K Y 2008 *Composites* A **39** 602–11
[25] Carballeira P and Haupert F 2010 *Polym. Composit.* **31** 1241–6
[26] Yang C Y, Lo C T, Bastawros A F and Narasimhan B 2009 *J. Mater. Res.* **24** 985–92
[27] Li J Y, Huang C and Zhang Q M 2004 *Appl. Phys. Lett.* **84** 3124–6
[28] Balazs A C, Emrick T and Russell T P 2006 *Science* **314** 1107–10